Title	Inefficiency in macromolecular transport of SCSbased microcapsules affects viability of primary human mesenchymal stem cells but not of immortalized cells
Author(s)	Sanz-Nogués, Clara; Horan, Jason; Thompson, Kerry; Howard, Linda; Ryan, Gerard; Kassem, Moustapha; O'Brien, Timothy
Publication Date	2015-05-01
Publication Information	Sanz-Nogués, Clara, Horan, Jason, Thompson, Kerry, Howard, Linda, Ryan, Gerard, Kassem, Moustapha, & O'Brien, Timothy. (2015). Inefficiency in macromolecular transport of SCS-based microcapsules affects viability of primary human mesenchymal stem cells but not of immortalized cells. Journal of Biomedical Materials Research Part A, 103(11), 3676-3688. doi: 10.1002/jbm.a.35493
Publisher	Wiley
Link to publisher's version	https://doi.org/10.1002/jbm.a.35493
Item record	http://hdl.handle.net/10379/15328
DOI	http://dx.doi.org/10.1002/jbm.a.35493

Inefficiency in macromolecular transport of SCS-based microcapsules affects viability of primary human mesenchymal stem cells but not of immortalized cells

Clara Sanz-Nogués[1], Jason Horan[2], Kerry Thompson[3], Linda Howard[1], Gerard Ryan[2], Moustapha Kassem[4,5] and Timothy O'Brien[1]*

[1] Regenerative Medicine Institute (REMEDI), Bioscience Research Building, National University of Ireland Galway, Newcastle Road, Galway, Ireland.

[2]Ziel Biopharma Ltd., Unit 4 Castletroy Park Business Centre, Castletroy, Ireland

[3] Centre for Microscopy and Imaging, Anatomy, National University of Ireland Galway, Newcastle Road, Galway, Ireland.

[4] Department of Endocrinology and Metabolism, University Hospital of Odense and University of Southern Denmark, Winsløwparken 25, DK-5000 Odense C, Denmark.

[5] Stem Cell Unit, Department of Anatomy, King Saud University (KSA), Riyadh 12372, Saudi Arabia.

ABSTRACT Microcapsules made of sodium cellulose sulphate (SCS) and poly-diallyl-dimethyl-ammonium chloride (pDADMAC) have been employed to encapsulate a wide range of established cell lines for several applications. However, little is known about the encapsulation of primary cells including human mesenchymal stem cells (hMSCs). Human MSCs are of interest in regenerative medicine applications due to pro-angiogenic, anti-inflammatory and immunomodulatory properties, which result from paracrine effects of this cell type. In the present work we have encapsulated primary hMSCs and hMSC-TERT immortalized cells and compared their behavior and *in vitro* angiogenic potential. We found that, although both cell types were able to secret angiogenic factors such as VEGF, there was a marked reduction of primary hMSC viability compared to hMSC-TERT cells when cultured in these microcapsules. Moreover, this applied to other primary cell cultures such as primary human fibroblasts but not to other cell lines such as human embryonic kidney 293 (HEK293) cells. We found that the microcapsule membrane had a molecular weight cut-off below a critical size, which caused impairment in the diffusion of essential nutrients and had a more detrimental effect on the viability of primary cell cultures compared to cell lines and immortalized cells.

KEYWORDS Microencapsulation, immunoisolation, sodium cellulose sulphate, mesenchymal stem cells and therapeutic angiogenesis.

INTRODUCTION

Human mesenchymal stem (stromal) cells (hMSCs) are a rare non-hematopoietic cell population present in bone marrow and other tissues capable of self-renewal and multi-lineage differentiation *in vitro*. They have the ability to form a variety of connective tissues including bone, fat and cartilage and they demonstrate specific surface antigen expression [(1),(2)]. Nevertheless, their therapeutic benefit is mostly related to the secretion of a wide range of paracrine factors, which may have anti-inflammatory, immunomodulatory and pro-angiogenic effects and may contribute to stimulation of local progenitor cells and tissue regeneration [(3)-(5)]. These properties may offer a clinical benefit for the treatment of inflammatory and ischemic conditions such as inflammatory bowel disease, coronary artery disease and peripheral arterial disease (PAD) [(6)]. Although results from current stem cell therapies using MSCs are encouraging, important limitations remain and major problems include the poor rate of engraftment and limited cell survival after transplantation. One of the reasons could be the susceptibility of MSCs (specifically allogeneic cells) to immune-mediated cell destruction, mainly through antibodies and complement proteins [(7)-(10)].

The use of biomaterials to encapsulate cells may overcome these problems and may enhance the therapeutic efficacy of stem cell transplantation. A combination of stem cell therapy and microencapsulation technology has three main potential benefits; a) immunoisolation of enclosed cells, b) cell retention at the transplanted site and c) long-term delivery of therapeutic factors.

Microcapsule systems with high mechanical strength and that induce low cytotoxicity and minimal inflammation, are advantageous. In this regard, microcapsules made of sodium cellulose sulphate (SCS) and poly-diallyl-dimethyl-ammonium chloride (pDADMAC) have been shown to be very stable and biocompatible [(11)-(13)]. Moreover, safety and proof of principle with this

63 approach have been demonstrated in a phase I/II clinical trial in patients with inoperable
64 pancreatic cancer [14],[15]. Several established cell lines including epithelial cells [16],[17],
65 fibroblasts [18], hybridoma cells [13],[19] islet cells [20],[21] and neural stem cells [22] have been
66 successfully encapsulated using this system. However, little is known about the behavior of
67 primary cells such as hMSCs encapsulated using this technology.

68 SCS-based microcapsules containing hMSCs may represent a system with potential for
69 enhancing persistence and efficacy in a broad range of conditions. One example would be in the
70 treatment of ischemic disorders by induction of therapeutic angiogenesis. In the present work, we
71 have characterized the morphology and chemical structure of SCS-pDADMAC microcapsules,
72 the cytotoxicity of the microcapsule components and the diffusion properties of its membrane.
73 Moreover, we have encapsulated primary hMSCs and hMSC-TERT immortalized cells [23],[24]
74 and studied their behavior and the *in vitro* angiogenic potential over a period of 14 days in
75 culture. In this study, we have also encapsulated primary human fibroblasts and the cell line
76 human embryonic kidney 293 (HEK293) to provide further data about the behavior of primary
77 *versus* cell lines.

78 **MATERIALS AND METHODS**

79 **Materials.** SCS (batch E12/1NEG2S13) with a sulphate-degree of substitution (ds) of 0.40
80 was purchased from Fraunhofer IAP (Potsdam, Germany) and Poly- (diallyl-dimethyl-
81 ammonium chloride) or pDADMAC of low molecular weight 100-200 kDa (Lot#
82 MKBK3094V) and ultra-low molecular weight <100 kDa (Lot# MKMF5290V) was obtained
83 from Sigma-Aldrich.

84 **Cell culture.** Primary hMSCs were isolated from human bone marrow (Lonza, Walkersville,
85 MD) and characterized based on the expression of CD105, CD73 and CD90 and lack of

expression of CD45, CD34, CD3, CD19, CD14 and HLA-DR and the tri-lineage differentiation capacity as stipulated by the International Society of Cellular Therapy [2] (Supporting Information Figure S1). A total of three different donors were used (*n=3*). These cells were cultured in standard complete medium consisting of α-MEM supplemented with 10% fetal bovine serum (FBS; Hyclone™, Thermo Scientific), 1% penicillin/streptomycin (Gibco, Invitrogen). Primary human (foreskin) fibroblasts (hFibroblasts) were obtained from ATCC and cultured in standard complete medium. HEK293 were cultured in D-MEM (high glucose) supplemented with 10% FBS, 1% penicillin/streptomycin and 2 mM L-Glutamine. The human MSC-TERT (hMSC-TERT) cell line has been established by ectopic expression of the catalytic subunit of human telomerase as previously described [23],[24]. These cells express all known markers of primary MSC and form ectopic bone and bone marrow organ when implanted *in vivo*. Human MSC-TERT cells were cultured with α-MEM supplemented with 10% FBS and 1% penicillin/streptomycin. Human Umbilical Vein Endothelial Cells (HUVECs) were obtained from Lonza and cultured in EBM-2 basal media (Lonza) containing EGM™-2 Bulletkit™ (serum and growth factors) (Lonza). All cells were maintained on a humidified incubator at 37ºC and 5% CO_2.

Procedure to encapsulate cells. For microcapsule preparation, 2% (w/v) SCS solution was prepared by dissolving 2 g SCS in 100 mL of sterile distilled water with 0.9% (w/v) of sodium chloride. This SCS solution was then filtered-sterilized (0.45 μm pore size). Cells were mixed with the 2% (w/v) SCS solution to give a final concentration of $5x10^6$ cells/mL. The SCS solution containing cells was passed through an encapsulator (Inotech encapsulator IE-50R, Switzerland) using a 200 μm nozzle. Droplets of equal size were formed and eventually fell into a well-stirred solution of sterile pDADMAC. The solution of pDADMAC was composed of

0.86% (w/v) of low molecular weight (100-200 kDa) and 0.06% (w/v) of ultra-low molecular weight (<100 kDa) species. The microcapsule shell was formed through polyelectrolyte complexation (PEC) of the anionic SCS with cationic pDADMAC polymer, resulting in the formation of stable liquid-core microcapsules containing cells, as previously described [11],[25]. The reaction time was adjusted to 4 min, and after that, microcapsules were washed 3 times with D-PBS (Gibco, Invitrogen) and 3 times with standard complete medium. All procedures were performed under sterile conditions. Microcapsules containing cells were stored in standard complete medium at 37ºC and 5% CO_2. Medium was changed every 2-3 days. The same conditions were used to generate microcapsules without cells.

Cell proliferation assay. For cell proliferation studies, primary hMSCs and hMSC-TERT cells were seeded at a density of 24,000 cells/well in a 12-well plate and cultured with complete medium, serum-free medium, 50K-depleted medium and 50K-concentrated medium for the culture period of 9 days. 50K-depleted medium was obtained by filtration of complete medium (α-MEM containing 10%FBS) with an ultra centrifugal filter device of 50K cut-off (Amicon® Ultracel-50K, Millipore) and 50K-concentrated media was obtained from the retentate volume. Both media were collected and used for culturing of cells. Protein content of media was analyzed by 15% SDS-PAGE and Silver Staining (Fermentas Life Science).

Characterization of microcapsules

Fourier transform infrared (FTIR) spectroscopy. The chemical structure of SCS, pDADMAC and polyelectrolyte complex (PEC) was analyzed by infrared spectroscopy. Analysis was performed on crude SCS (solid form) and pDADMAC (20% (v/v) solution, Sigma-Aldrich). For PEC membrane formation, a solution of 1% (w/v) pDADMAC was added to 2% (w/v) SCS until polymerization occurred and an insoluble compound was formed. The spectra were acquired on

an FTIR-8300 spectrophotometer with an average of 20 scans, a resolution of 4 cm^{-1} and a wavenumber range of 600-4000 cm^{-1} at ambient temperature.

Microscopic analysis of microcapsules. The diameter of 50 microcapsules from three independent encapsulation procedures was measured using confocal laser scanning microscopy (CLSM; Zeiss LSM 510 Axiovert Inverted Confocal Microscope) to determine microcapsule size distribution and reproducibility. Scanning electron microscopy (SEM) was employed to study the ultrastructure of microcapsules. For visualization of the microcapsules' outer surface and membrane cross-section, microcapsules were dehydrated through graded ethanol, sputter-coated with colloidal gold and observed with Hitachi S2600N Variable Pressure Scanning Electron Microscope. For images created using Back Scattered Electron Mode (BES) – the Back Scattered Electron detector was inserted into the system. In this case, microcapsules did not undergo a dehydration process and instead, they were directly visualized. The beam size was increased to at least 80, a higher kV was also used (20-25kV) and pressure was set at between 50-80 Pascals (Pa).

Cytoperformance of encapsulated cells

Determination of viability and metabolic activity. Cell viability on days 0, 1, 3, 7 and 14 days post-encapsulation was assessed using the LIVE/DEAD® viability/cytotoxicity assay (Molecular probes, Invitrogen) as recommended by the manufacturer. Microcapsules containing cells were visualized under CLSM (Zeiss LSM 510 Axiovert Inverted Confocal Microscope) using the excitation/emission wavelengths of ~528nm/~617nm (red fluorescence) and ~495 nm/~515 nm (green fluorescence). Scans throughout the whole microcapsule were taken using a step size of 5μm. These scans were then projected onto 2D-plane (z projection) using the software provided. As a control, encapsulated hMSCs were killed using pure ethanol, stained with LIVE/DEAD®

dyes and observed using CLSM. The metabolic activity of encapsulated cells immediately after encapsulation and on days 3, 7 and 14 post-encapsulation, was assessed using AlamarBlue® assay. AlamarBlue® (10% of the volume of the well) was added to each well containing 30 ± 3 microcapsules (5 experimental replicas in 96-well plates) and incubated for 21 h at 37ºC protected from the light. After incubation, 2 aliquots of 100µl per well were transferred to a 96-well plate. Absorbance was measured at 550nm with wavelength correction at 595nm using a microplate reader (Victor3 1420 multilabel plate counter). Results were expressed as mean ± SD from 3 independent encapsulation processes.

Cytoskeleton organization. Samples of microcapsules containing cells were collected at days 0, 3, 7 and 14, fixed in 4% paraformaldehyde in D-PBS for 20 min and permeabilized with 0.1% TritonX-100 (Sigma-Aldrich) for 5 min. The nucleus of the encapsulated cells was stained with 0.25mg/mL of Propidium Iodide (PI) (Sigma-Aldrich) for 10 min. Cell cytoskeleton was stained for F-actin with 50µg/mL Phalloidin-FITC (Sigma-Aldrich) for 45 min at room temperature protected from light. Microcapsules were visualized using CLSM (Zeiss LSM 510 Axiovert Inverted Confocal Microscope) using excitation and emission wavelengths of ~495 nm/~515 nm (green fluorescence) and ~528nm/~617nm (red fluorescence), respectively.

Cell localization. Localization of cells inside the microcapsules was investigated using CLSM (Zeiss LSM 510 Axiovert Inverted Confocal Microscope) and LIVE/DEAD® dyes as above. Scans throughout the whole microcapsule were taken using a step size of 5µm and images were projected to an orthographic projection.

***In vitro* cytotoxicity assays.** The biological response of primary hMSCs to microcapsule material was assessed as stipulated by the International Organization for Standardization, ISO 10993-5:2009(E). Briefly, 5,000 cells/well in 48-well plates were cultured for 48h in direct

contact with sterile empty microcapsules (direct contact) and with extracts of the microcapsule device through diffusion (indirect contact). In addition, cells were incubated with 2% and 4% (w/v) SCS solution re-suspended in complete medium at ratios of 1:3 and 2:3 (SCS:media). In the three experiments, cytotoxicity was assessed 48h later using an AlamarBlue® assay, as recommended by the manufacturer. Furthermore, primary hMSCs were cultured in suspension with a solution containing sterile empty microcapsules in serum-free conditions. The ability of primary hMSCs to spread on the outer microcapsule membrane was studied using CLSM at the time of cell seeding and 24h after, using transmitted laser light and LIVE/DEAD® reagents (z-projection and orthographic projection).

Molecular weight cut-off of microcapsule membrane. The molecular weight cut-off (MWCO) of the microcapsule membrane was determined by incubating 40-50 microcapsules in 1 mL of D-PBS, supplemented with 0.5 mg/mL of FITC-labeled dextran (10, 20 and 70 kDa; Sigma-Aldrich), 40 µg/mL of FITC-coupled chicken anti-rabbit IgG (or IgY, 180kDa; Abcam) and 0.5 mg/mL of FITC-coupled BSA (66.5 kDa, Sigma-Aldrich). After 20h, FITC-fluorescence inside and outside of the microcapsules was determined by CLSM (Zeiss LSM 510 Axiovert Inverted Confocal Microscope). The distribution of fluorescence intensity was obtained by performing a linear scan of microcapsules using the CLSM software.

***In vitro* angiogenic potential of encapsulated cells.** Levels of Vascular Endothelial Growth Factor (VEGF) released from encapsulated cells were assessed by ELISA (R&D Systems) as recommended by the manufacturer. Seven days after encapsulation, microcapsules containing cells were re-suspended in fresh complete medium and samples of conditioned medium were collected at 24h, 48h and 72h for VEGF quantification. Similarly, VEGF levels were quantified from the conditioned medium of non-encapsulated cells (50,000 cells/well) cultured for 24h, 48h

and 72h. The ability of encapsulated cells to secrete factors that induce the formation of tube-like structures by HUVECs was investigated using a matrigel tube formation assay. After 7 days of culture, microcapsules containing cells were incubated with EBM medium (without addition of serum and growth factors) for 48h, after which time, the conditioned medium was generated and collected. Growth factor reduced matrigel basement membrane (BD Matrigel Matrix Growth Factor Reduced, BD Bioscience) was thawed on ice at 4ºC overnight. A thin layer (110µL/well) was added to 48-well plates and allowed to solidify at 37ºC. HUVECs ($2.5x10^4$ cells) were re-suspended with the appropriated media (3 experimental replicas: conditioned medium from encapsulated cells, EBM-2 medium for negative control and EGM-2 medium for positive control). Media containing HUVECs were added on top of the matrigel and incubated for 14h at 37ºC. After incubation, four pictures per well were taken at random and a quantitative measurement of tube-like structures was carried out and normalized to the positive control. Tubules were considered as structures that were at least 4 times the length of a cell.

Statistical analysis. Statistical analysis of the results was performed using Graphpad Prism (Graphpad Prism 5 Software). The D'Agostino&Pearson test was used for testing the normal distribution of the samples. The results of multiple observations are represented as mean ± standard deviation (SD) ($n=3$). For two-sample data analysis, unpaired Student's *t*-test was performed. For multivariate data analysis, group differences were assessed with one-way analysis-of-variance (ANOVA) with corresponding multiple comparison test, which are specified in the legend of each figure. Differences were considered statistically significant when *p* values were lower than 0.05.

RESULTS

Chemical and morphological characterization of microcapsules. Microcapsules made of SCS and pDADMAC are liquid-core microcapsules, which are formed when two oppositely charged polyelectrolytes (i.e. anionic SCS and cationic pDADMAC) interact in an aqueous solution. As a consequence, a solid-like precipitate called polyelectrolyte complex (PEC) is formed at the droplet surface, which acts as a semipermeable membrane [26]. This semipermeable membrane may permit bidirectional diffusion of nutrients, oxygen and secreted factors but prevents the entry of bigger molecules (i.e. antibodies) and host immune cells (Fig. 1A). In the present work, we have characterized the morphology and structure of the SCS-pDADMAC microcapsules. Scanning electron microscopy (SEM) was used to study the overall microcapsule ultrastructure. Microcapsules made of SCS and pDADMAC are composed of a liquid-core of unreacted SCS polyelectrolyte enveloped by a semipermeable membrane made of PEC (Fig. 1B). SCS-pDADMAC microcapsules represent an osmotically interactive system [25] and osmotic pressure differences may cause changes in capsule volume by movement of water. In figure 1B, microcapsules were visualized under SEM using the BSE mode to observe the natural structure of microcapsules. These samples were not dehydrated through graded ethanol and appeared as spherical structures with a smooth surface. It is proposed that the microcapsule's liquid-core diffused out when they were subjected to the dehydration process during the preparation for SEM visualization, and as a result they appeared as collapsed spherical structures (Fig. 1C). In this image it is suggested that the dehydrated microcapsule is entirely formed by PEC membrane.

FTIR spectrum was used to confirm the naïve structures of SCS and pDADMAC and the formation of the membrane by PEC after polymerization (Fig. 1D). The most characteristic peaks in the SCS spectrum are the bridge oxygen (C-O-C ether) and the C-OH stretching bands

observed as multiple peaks in the region of 990-1150cm^{-1}, and the strong bands of S=O and –SO_3^- at 1217cm^{-1} and C-O-S at 808cm^{-1}. In the pDADMAC spectrum, a broad peak at 2100cm^{-1}, due to the –CN stretching, and a peak at 1473cm^{-1} attributed to the -CH_3 groups, were also identified. PEC membrane formation was confirmed by its solid-like structure and insoluble character compared to the unreacted liquid SCS and pDADMAC. The PEC spectrum includes peaks at 2100cm^{-1} from –CN stretching and multiple peaks at the region of 990-1150cm^{-1} from the C-O-C and C-OH groups.

Finally, microcapsule size distribution and reproducibility was studied by measuring the diameter of 50 microcapsules from 3 independent encapsulation processes. SCS-pDADMAC microcapsules produced by the vibrational technology are known to have a narrow size distribution [27]. Microcapsules produced with the conditions described in the materials and methods are highly reproducible and have a diameter of 556.99 ± 30.33μm with a narrow size distribution (Fig. 1E).

Survival of primary hMSCs is compromised after encapsulation. Viability of encapsulated primary hMSCs was measured after encapsulation and on days 1, 3, 7 and 14 using LIVE/DEAD® viability/cytotoxicity assay. Primary hMSCs survived the encapsulation process, as they exhibited green fluorescence immediately after encapsulation (day 0). However, viability over time was compromised as was indicated by the appearance of red fluorescent cells (Fig. 2A). Metabolic activity measurements using AlamarBlue® assay confirmed these results (Fig. 2B). We found a pronounced reduction of metabolic activity of 64.44 ± 15.56% by day 3 compared to day 0, and this further decreased by day 7.

The localization of cells within the microcapsules was investigated using LIVE/DEAD® dyes and CLSM. Primary hMSCs remained in single cells and were distributed throughout the liquid-

core of the microcapsule immediately after encapsulation (Fig. 2C). However, we observed that cells started to clump together a few hours after encapsulation, and they remained in clumps until day 14. Furthermore, we observed that these cells failed to spread and localized close to the inner microcapsule membrane (Fig. 2C and Video S1).

The morphology of hMSCs inside the SCS-based microcapsules was assessed by CLSM and staining of F-actin and cell nuclei with Phalloidin-FITC (green) and PI (red), respectively (Fig. 2D). Primary hMSCs had a rounded morphology immediately after encapsulation and formed clumps about 70-80 μm in diameter by day 3. Cells remained in a round shape within the clumps, with poor cytoplasmic extensions around the cells (Fig. 2D). Transmitted laser light and LIVE/DEAD® dyes were used to visualize the conformation of the cell clumps (Supporting Information Fig. S2). Primary hMSCs clumps were initially formed by healthy cells, although considerable cell death was detectable 3 days after encapsulation. At 14 days, these cell clumps were mainly formed by a small core of viable cells (green) surrounded by dead cells (red).

Microcapsule material is not cytotoxic to primary hMSCs. The cytotoxicity of microcapsule components to primary hMSCs was assessed 48 h after first contact with the material (by direct or indirect contact), using an AlamarBlue® assay (Fig. 3A). Results showed that neither PEC, which forms the microcapsule membrane (Fig. 3Ai), nor extracts released by microcapsules, which may contain residual amount of polyelectrolyte (Fig. 3Aii), had a cytotoxic effect on primary hMSCs. Moreover, metabolic activity of primary hMSCs was maintained in cells cultured in direct contact with a solution of unreacted SCS (which forms the liquid-core of the microcapsules) at concentrations of 2% and 4% (w/v) (Fig. 3Aiii). Interestingly, we found that primary hMSCs were able to spread on the outer layer of the microcapsule membranes when cultured in serum-free conditions for 24 h (Fig. 3B).

293 **Immortalized hMSCs survive after microencapsulation.** Results from LIVE/DEAD® assay
294 showed that immortalized hMSC-TERT cells remained viable during the culture period tested
295 (14 days), as most of the cells were stained with Calcein AM (Fig. 4A). Likewise, the
296 AlamarBlue® assay showed that encapsulated hMSC-TERT cells maintained their metabolic
297 activity during the 14 days (Fig. 4B). Human MSC-TERT cells also formed clumps, however,
298 they were mainly composed of healthy cells stained with Calcein AM (green). These clumps
299 were able to increase in size with little cell death (Supporting Information Fig. S2). Human
300 MSC-TERT cells were found to move towards the inner microcapsule membrane similarly to
301 primary hMSCs (Fig. 4C). Furthermore, hMSC-TERT cells were able to proliferate as seen by
302 the higher cell density found inside of the microcapsule at day 14 compared to day 0 (Fig. 4A).
303 Cells were able to spread on the inner membrane of the microcapsule as seen in orthographic
304 projection in figure 4C and Video S2. Results from F-actin and cell nuclei staining showed that
305 hMSC-TERT cells formed compact and well-organized clumps, which had different shapes (Fig.
306 4D). These cell clumps grew in size forming very dense cellular structures 14 days after
307 encapsulation.
308 In order to provide further data on the behavior of primary cells and cell lines, we encapsulated
309 other cell types including primary human fibroblasts and HEK293 cells (Supporting Information
310 Fig. S3). Results from LIVE/DEAD® staining showed that a reduction in cell viability occurred
311 in primary human fibroblasts but not in HEK293 cells.
312 **Diffusion of macromolecules is impeded by the microcapsule membrane.** The ultrastructure
313 of the microcapsule membrane was determined by SEM. The microcapsule membrane appeared
314 to be a very dense, smooth and compact structure, and large diffusion channels (i.e. pores) were
315 not observed (Fig. 5A). The diffusion of 10, 20 and 70 kDa FITC-labeled dextrans, FITC-

316 coupled IgY (180kDa) and FITC-coupled BSA (66.5kDa) across the microcapsule membrane
317 was investigated (Fig. 5B). Results showed that small molecules such as 10 kDa dextrans were
318 able to permeate easily, while 20 kDa dextrans were able to permeate to an extent, as seen by a
319 reduced fluorescence inside the microcapsules. Moreover, its diffusion did not improve at 96h
320 (Supporting Information Fig. S4). Furthermore, BSA (66.5kDa), one of the most abundant
321 globular proteins present in the FBS employed for the culture of cells, was not able to penetrate
322 the microcapsule membrane and appeared adsorbed at the outer microcapsule membrane.
323 Finally, large molecules including antibodies (i.e. 70kDa dextran and 180kDa IgY) were also not
324 able to permeate the microcapsule membrane.

325 **Macromolecules present in complete medium have an impact in the growth of cells.**
326 Macromolecules present in complete medium were depleted based on size using a 50K-filter
327 device. Protein content of media was analyzed by SDS-PAGE. Results showed that complete
328 medium included proteins ranging from <1 to >180 kDa, while no protein content was detected
329 by SDS-PAGE in the serum-free medium (Fig. 6A). We found that macromolecules larger than
330 ~70kDa were retained in the concentrate while the concentration of proteins <50kDa were
331 diminished as a consequence of the 50K-filtration step. This fractionation would mimic a
332 possible delay and/or impediment on the entrance of macromolecules from the medium into the
333 microcapsules.

334 Primary hMSCs and MSC-TERT cells were incubated with completed medium, serum-free
335 medium and 50K-depleted medium, and cell proliferation was assessed 9 days after. Results
336 showed that primary hMSCs failed to proliferate in the 50K-depleted medium and in serum-free
337 conditions (Fig. 6B). Conversely, hMSC-TERT cells were able to proliferate in both serum-free
338 conditions and 50K-depleted medium, although their growth was slower compared to the

complete medium (Fig. 6B). We found that hMSC-TERT cells cultured in 50K-depleted medium underwent ~9-fold increase in cell number compared to day 0. However, primary hMSCs showed a decrease in cell number when compared to day 0 (Fig. 6C).

Encapsulated cells secrete angiogenic factors. Primary hMSCs and hMSC-TERT cell line are known to secret angiogenic factors [3],[5],[28],[29]. The release of functional angiogenic factors from the encapsulated cells was studied using a matrigel tube formation assay [30]. We found that the conditioned medium (CM) from encapsulated primary hMSCs and hMSC-TERT cells was able to induce tube-like structures in HUVECs (Fig. 7A-B). Moreover, ELISA quantification of VEGF levels from non-encapsulated cells showed that both cell types were able to secrete this angiogenic protein. However, the release of VEGF by hMSC-TERT cells increased over time and at 72h (2374.42 ± 398.85 pg/mL) it was greater than primary hMSCs (1223.86 ± 684.56 pg/mL), probably due to the higher proliferation rate of this cell type (Supporting Information Fig. S5). Encapsulated primary hMSCs and hMSC-TERT cells also secreted VEGF (Fig. 7C), but again, hMSC-TERT cells performed better in terms of both quantity and duration of protein secreted.

DISCUSSION

Our results indicate the potential of SCS-pDADMAC microcapsules as devices for long-term delivery of angiogenic factors secreted by the encapsulated cells, while simultaneously protecting the cells from the contact with antibodies. This would be valuable for allogeneic stem cell transplantation in the field of therapeutic angiogenesis. However, we have found that the survival of primary cells is compromised after encapsulation.

To our knowledge, SCS-based microcapsule systems have been mainly employed for the encapsulation of established cell lines [13]-[22]. However, the use of cell lines may be a concern for

362 the regulatory bodies when designing clinical trials, in particular, immortalized cells that are able
363 to form tumors *in vivo.* For this reason, our interest focused on the encapsulation of primary
364 human cells such as MSCs, which are of interest in many clinical applications. In the present
365 work, we have also investigated the behavior of other primary cell types such as human
366 fibroblasts, and two cell lines including hMSC-TERT cells and HEK293 cells, for comparative
367 purposes.

368 Our results showed that the viability of primary cells such as hMSCs and hFibroblasts
369 encapsulated in this device was limited compared to the performance of established cell lines
370 such as hMSC-TERT and HEK293 cells. Likewise, hMSC had a reduced metabolic activity over
371 the 14 days of culture compared to hMSC-TERT cells. This observation suggests that primary
372 cells may find some elements of microcapsule environment detrimental whereas their
373 immortalized counterpart is able to survive in these conditions. Nevertheless, we found that
374 microcapsule material was not cytotoxic to primary hMSCs by either direct or indirect contact.

375 Intriguingly, we found that hMSC-TERT cells had extensive proliferation by day 14, and cells
376 occupied about 50% of the microcapsule inner membrane. Uncontrolled proliferation from
377 immortalized cells could be worrisome from a safety point of view. Although these cells may be
378 protected from the host immune system by the microcapsule membrane, an uncontrolled
379 proliferation of these cells could cause a rupture of the microcapsule and release of the cells,
380 which could compromise the health of the patient. However, we did not observe an extensive
381 proliferation by the encapsulated primary hMSCs during the 14 days studied.

382 CLSM was used to study the localization of cells after encapsulation. These results showed
383 that primary hMSC were distributed as a single cell suspension throughout the microcapsule
384 immediately after encapsulation and remained with in rounded morphology for 14 days.

However, we observed a movement of cells out of the center towards the membrane, where nutrients and oxygen might be more readily available to cells, as previously reported [11]. We suggest that this effect may be more likely to be caused by gravitational forces that pull the cells towards the bottom of the microcapsule, as the liquid-core of these microcapsules may not support the interaction or attachment of cells. Moreover, we observed that primary hMSC had a rounded morphology with no cytoplasmic elongations (which may be indicative of some kind of interaction with the material), suggesting that cells do not interact with the liquid-core of the microcapsules. In contrast, PEC that forms the microcapsule membrane, a solid-like precipitate [26], may provide better support for cell anchorage than the liquid-core of the microcapsules.

In this regard, it is important that the inner layer of the microcapsule membranes provides the correct adhesion signals to cells. Primary hMSCs are anchorage dependent cells, and as in many other cells types, they require integrin-mediated adhesion to extracellular matrix (ECM) proteins to display optimal metabolic functionality and viability. When this does not occur, cells may die through a mechanism called *anoikis*, or anchorage-dependent cell death [31],[32]. In contrast, some immortalized cell types such as hMSC-TERT cells may exhibit anchorage-independent growth, as determined by the soft agar colony assay [33]. We investigated whether primary hMSC were capable of spreading on the outer membrane of the microcapsule, even when cells were cultured under serum-free conditions (to avoid the presence of serum-derived adhesion molecules such as fibronectin [34]). Interestingly, we found that primary hMSCs were able to spread on the outer microcapsule membrane suggesting that: a) PEC that forms the microcapsule membrane is not cytotoxic, and b) the microcapsule membrane, although not made of natural extracellular matrix components, may provide adhesion signals to primary hMSCs. Interestingly, it has been previously shown that the outer and the inner membrane of the SCS-pDADMAC microcapsules

408 have similar surface composition [35],[36]. Although we found that hMSC-TERT cells were able to
409 spread to some extent on the inner membrane of the microcapsule, we observed that primary
410 hMSCs failed to do so. We hypothesized that *anoikis*, or anchorage-dependent cell death related
411 to the structure of the microcapsule membrane may not be the main (or the only) cause of the
412 reduced viability in primary cells. Nevertheless, primary hMSCs may require other attachment
413 and spreading factors for long-term survival that the microcapsule membrane may not provide.
414 Immortalized cells may overcome this possibly due to up-regulation of other cell survival
415 mechanism. In this study we have not investigated whether the inner membrane provided
416 attachment signals to the cells (e.g. *via* integrin expression by encapsulated cells).
417 Furthermore, membrane pores below a critical size may cause inefficient diffusion and delay in
418 the transport of substances into the microcapsule, which could negatively affect the growth and
419 survival of the encapsulated cells. Membranes formed by SCS and pDADMAC crosslinking are
420 known to have a very low molecular weight cut-off (MWCO). For instance, Zhang et al. showed
421 that SCS-pDADMAC microcapsules prepared with their conditions had a MWCO of ~ 14k Da,
422 meaning that proteins larger than 14 kDa hardly permeate through the membrane [37] Dautzenber
423 et al. characterized the membrane cut-off limits of SCS-pDAMAC microcapsules prepared with
424 different pDADMAC solutions with mass portions of size fractions >10kDa, and they found that
425 the cut-off range corresponded to a molecule with R_h ~ 1.9 nm (equal to a globular protein of
426 about 18k Da) [38]. According to Dautzenber et al., size exclusion properties may be influenced
427 by several variables during the capsule formation including the concentration of pDADMAC and
428 its molecular weight, the polymerization time and the presence of monovalent salt in the
429 pDADMAC solution [25],[26],[38]. Therefore, in this study, we have characterized the properties of
430 the PEC membrane made with the conditions described in the experimental section. SEM

analysis of the microcapsule membrane showed that this was formed by a very compact structure with no visible large pores. However, the dehydration step performed during the sample preparation could have had a detrimental effect on the structure of the membrane's pores. Therefore, we studied the microcapsule membrane permeability properties in a functional manner (e.g. by the ability of molecules of different molecular weight to diffuse into the microcapsule). Results from this permeability study showed that only small molecules (i.e. 10 kDa dextran) were able to freely permeate the microcapsule membrane, while 20 kDa dextran permeated only to an extent and BSA (66.5 kDa) appeared absorbed to the outer membrane. Moreover, we demonstrated that large molecules such as antibodies (i.e. 70k Da dextran and 180 kDa IgY) were not able to permeate and therefore, cells could be protected from an antibody-mediated immune attack.

Table 1 shows the correspondent hydrodynamic radius (R_h) of some molecules as a reference for permeability estimation. The R_h is employed for comparing the size of proteins, which have different molecular shapes (i.e. dextrans or globular proteins). It is defined as the radius of a hypothetical hard sphere that diffuses with the same speed as the molecule under examination and it is closely related to solvent motility. From the permeability experiments, we can stipulate that the pore size of the microcapsule membrane may correspond, approximately, with the size of a molecule with R_h between 3.2 nm and 3.48 nm. Therefore, we would expect that small molecules such as glucose, most cytokines and growth factors (i.e. VEGF which has a molecular weight of 45 kDa and a calculated R_h of 3.02 nm [39]) present in the culture medium and/or released by the encapsulated cells would be able to diffuse through the microcapsule membrane. In this regard, we could observe a release of angiogenic factors, including VEGF, from encapsulated cells after 7 days in culture, as determined by the matrigel tubule formation assay

and quantification of VEGF levels from the conditioned medium. We found that hMSC-TERT cells secreted higher levels of VEGF than primary hMSCs probably due to a higher viability of these encapsulated cells at that chosen time point.

FBS is used as an almost universal growth supplement in cell culture media for most types of human and animal cells. It is composed of low and high molecular weight biomolecules including hormones, vitamins, carbohydrates and proteins including serum proteins, growth factors and cytokines, transport proteins, attachment and spreading factors and enzymes, which are vital for the attachment, growth and proliferation of cells [34],[40]. We investigated whether primary hMSCs and hMSC-TERT cells were able to grow in FBS-free medium or in medium depleted of macromolecules >50 kDa (50kD-depleted medium). We found that primary hMSCs were more sensitive to serum-free conditions than MSC-TERT cells, and that they need macromolecules (i.e. < 50 kDa) present in the serum for survival and proliferation. For instance, primary hMSCs may need macromolecules such as transferrin (80k Da) (important for transferring iron to the cells [34]) and serum albumin (66.5 kDa) (a potent antioxidant especially in serum-starved conditions [41],[42]) for optimal proliferation and survival. In contrast, the growth and viability of immortalized cell lines such as hMSC-TERT cells was less compromised by these conditions, as these cells proliferated even in the absence of serum.

Based on our results, we concluded that liquid-core microcapsules must have a membrane pore size that allows the entrance of proteins >50 kDa in order to support primary hMSCs viability. However, if immunoprotection of enclosed cells is of interest, these microcapsules must have a pore size <150 kDa (e.g. IgG). Nonetheless, finding a correct balance could be challenging.

Corresponding Author * Timothy O'Brien: timothy.obrien@nuigalway.ie

Conflict of Interest Disclosure No benefit of any kind will be received either directly or indirectly by the author(s).

ACKNOWLEDGMENTS

This work was supported by Science Foundation of Ireland (SFI), Strategic Research Cluster (SRC), Grant No. 09/SRC/B1794 and co-funded by the European Regional Development Fund (ERDF). The authors acknowledge the facilities and technical assistance of Pierce Lalor from the Centre for Microscopy & Imaging at the National University of Ireland Galway (www.imaging.nuigalway.ie), a facility that is funded by NUIG and the Irish Government's Programme for Research in Third Level Institutions, Cycles 4 and 5, National Development Plan 2007-2013.

REFERENCES

1. Barry FP, Murphy JM. Mesenchymal stem cells: clinical applications and biological characterization. Int J Biochem Cell Biol. 2004;36:568–84.
2. Dominici M, Le Blanc K, Mueller I, Slaper-Cortenbach I, Marini F, Krause D, Deans R, Keating A, Prockop D, Horwitz E. Minimal criteria for defining multipotent mesenchymal stromal cells. The International Society for Cellular Therapy position statement. Cytotherapy. 2006;8:315–7.
3. Kinnaird T, Stabile E, Burnett MS, Lee CW, Barr S, Fuchs S, Epstein SE. Marrow-derived stromal cells express genes encoding a broad spectrum of arteriogenic cytokines and promote in vitro and in vivo arteriogenesis through paracrine mechanisms. Circulation Research. 2004;94:678–85.
4. Hoogduijn MJ, Popp F, Verbeek R, Masoodi M, Nicolaou A, Baan C, Dahlke M-H. The immunomodulatory properties of mesenchymal stem cells and their use for immunotherapy. Int Immunopharmacol. 2010;10:1496–500.
5. Burlacu A, Grigorescu G, Rosca A-M, Preda MB, Simionescu M. Factors secreted by mesenchymal stem cells and endothelial progenitor cells have complementary effects on angiogenesis in vitro. Stem Cells Dev. 2013;22:643–53.
6. Liew A, O'Brien T. Therapeutic potential for mesenchymal stem cell transplantation in critical limb ischemia. Stem Cell Research & Therapy. 2012;3:28.
7. Eliopoulos N, Stagg J, Lejeune L, Pommey S, Galipeau J. Allogeneic marrow stromal cells are immune rejected by MHC class I- and class II-mismatched recipient mice. Blood. 2005;106:4057–65.
8. Moloney TC, Dockery P, Windebank AJ, Barry FP, Howard L, Dowd E. Survival and Immunogenicity of Mesenchymal Stem Cells From the Green Fluorescent Protein Transgenic Rat

in the Adult Rat Brain. Neurorehabilitation and Neural Repair. 2010;24:645–56.
9. Zangi L, Margalit R, Reich-Zeliger S, Bachar-Lustig E, Beilhack A, Negrin R, Reisner Y. Direct imaging of immune rejection and memory induction by allogeneic mesenchymal stromal cells. Stem Cells. 2009;27:2865–74.
10. Hofmann M, Wollert KC, Meyer GP, Menke A, Arseniev L, Hertenstein B, Ganser A, Knapp WH, Drexler H. Monitoring of bone marrow cell homing into the infarcted human myocardium. Circulation. 2005;111:2198–202.
11. Dautzenberg H, Schuldt U, Grasnick G, Karle P, Müller P, Löhr M, Pelegrin M, Piechaczyk M, Rombs KV, Günzburg WH, Salmons B, Saller RM. Development of cellulose sulfate-based polyelectrolyte complex microcapsules for medical applications. Ann N Y Acad Sci. 1999;875:46–63.
12. Löhr J-M, Saller R, Salmons B, Günzburg WH. Microencapsulation of genetically engineered cells for cancer therapy. Meth Enzymol. 2002;346:603–18.
13. Pelegrin M, Marin M, Noël D, Del Rio M, Saller R, Stange J, Mitzner S, Günzburg WH, Piechaczyk M. Systemic long-term delivery of antibodies in immunocompetent animals using cellulose sulphate capsules containing antibody-producing cells. Gene Ther. 1998;5:828–34.
14. Löhr M, Kroger JC, Hoffmeyer A, Freund M, Hain J, Holle A, Knofel WT, Liebe S, Nizze H, Renner M. Safety, feasibility and clinical benefit of localized chemotherapy using microencapsulated cells for inoperable pancreatic carcinoma in a phase I/II trial. Cancer Ther. 2003;1:121–31.
15. Löhr M, Hoffmeyer A, Kröger J, Freund M, Hain J, Holle A, Karle P, Knofel WT, Liebe S, Müller P, Nizze H, Renner M, Saller RM, Wagner T, Hauenstein K, Günzburg WH, Salmons B. Microencapsulated cell-mediated treatment of inoperable pancreatic carcinoma. Lancet. 2001;357:1591–2.
16. Karle P, Müller P, Renz R, Jesnowski R, Saller R, Rombs von K, Nizze H, Liebe S, Günzburg WH, Salmons B, Löhr M. Intratumoral injection of encapsulated cells producing an oxazaphosphorine activating cytochrome P450 for targeted chemotherapy. Adv Exp Med Biol. 1998;451:97–106.
17. Müller P, Jesnowski R, Karle P, Renz R, Saller R, Stein H, PÜSCHEL K, Rombs K, Nizze H, Liebe S. Injection of Encapsulated Cells Producing an Ifosfamide-Activating Cytochrome P450 for Targeted Chemotherapy to Pancreatic Tumors. Ann N Y Acad Sci. Wiley Online Library; 1999;880:337–51.
18. Saller RM, Indraccolo S, Coppola V, Esposito G, Stange J, Mitzner S, Amadori A, Salmons B, G nzburg WH. Encapsulated cells producing retroviral vectors forin vivo gene transfer. J Gene Med. 2002;4:150–60.
19. Pelegrin M, Marin M, Oates A, Noël D, Saller R, Salmons B, Piechaczyk M. Immunotherapy of a Viral Disease by in VivoProduction of Therapeutic Monoclonal Antibodies. Human Gene Therapy. 2000;11:1407–15.
20. Schaffellner S, Stadlbauer V, Stiegler P, Hauser O, Halwachs G, Lackner C, Iberer F, Tscheliessnigg KH. Porcine islet cells microencapsulated in sodium cellulose sulfate. J Am Coll Cardiol. 2005;37:248–52.
21. Stadlbauer V, Stiegler PB, Schaffellner S, Hauser O, Halwachs G, Iberer F, Tscheliessnigg KH, Lackner C. Morphological and functional characterization of a pancreatic beta-cell line microencapsulated in sodium cellulose sulfate/poly(diallyldimethylammonium chloride). Xenotransplantation. 2006;13:337–44.
22. Dangerfield JA, Salmons B, Corteling R, Abastado J-P, Sinden J, Günzburg WH, Brandtner EM. The Diversity of Uses for Cellulose Sulphate Encapsulation. Brandtner EM, Dangerfield JAIn: editors, editor. Bioencapsulation of living cells for diverse medical applications. Bentham Science Publishers; 2013.
23. Abdallah BM, Haack-Sørensen M, Burns JS, Elsnab B, Jakob F, Hokland P, Kassem M.

560 Maintenance of differentiation potential of human bone marrow mesenchymal stem cells
561 immortalized by human telomerase reverse transcriptase gene despite of extensive proliferation.
562 Biochem Biophys Res Commun. 2005;326:527–38.
563 24. Simonsen JL, Rosada C, Serakinci N, Justesen J, Stenderup K, Rattan SIS, Jensen TG, Kassem M.
564 Telomerase expression extends the proliferative life-span and maintains the osteogenic potential of
565 human bone marrow stromal cells. Nat Biotechnol. Nature Publishing Group; 2002;20:592–6.
566 25. Dautzenberg H, Lukanoff B, Eckert U, Tiersch B, Schuldt U. Immobilisation of biological matter
567 by polyelectrolyte complex formation. Berichte der Bunsengesellschaft für physikalische Chemie.
568 Wiley Online Library; 1996;100:1045–53.
569 26. Dautzenberg H, Arnold G, Lukanoff B, Eckert U, Tiersch B. Polyelectrolyte complex formation at
570 the interface of solutions. Springer; 1996;:149–56.
571 27. Heinzen C, Berger A, Marison IW. Use of Vibration Technology for Jet Break- up for
572 Encapsulation of Cells and Liquids in Monodisperse Microcapsules. Nedovic V, R WIn: editors,
573 editor. *Fundamentals of Cell Immobilisation Technology*. Kluwer Academic Publishers; 2004.
574 28. Duffy GP, Ahsan T, O'Brien T, Barry F, Nerem RM. Bone marrow-derived mesenchymal stem
575 cells promote angiogenic processes in a time- and dose-dependent manner in vitro. Tissue
576 engineering Part A. 2009;15:2459–70.
577 29. Burns JS, Kristiansen M, Kristensen LP, Larsen KH, Nielsen MO, Christiansen H, Nehlin J,
578 Andersen JS, Kassem M. Decellularized Matrix from Tumorigenic Human Mesenchymal Stem
579 Cells Promotes Neovascularization with Galectin-1 Dependent Endothelial Interaction. PLoS
580 ONE. Public Library of Science; 2011;6:e21888.
581 30. Kubota Y, Kleinman HK, Martin GR, Lawley TJ. Role of laminin and basement membrane in the
582 morphological differentiation of human endothelial cells into capillary-like structures. J Cell Biol.
583 1988;107:1589–98.
584 31. Benoit DSW, Tripodi MC, Blanchette JO, Langer SJ, Leinwand LA, Anseth KS. Integrin-linked
585 kinase production prevents anoikis in human mesenchymal stem cells. J Biomed Mater Res.
586 2007;81A:259–68.
587 32. Frisch SM, Screaton RA. Anoikis mechanisms. J Am Coll Cardiol. 2001;13:555–62.
588 33. Burns JS, Abdallah BM, Guldberg P, Rygaard J, Schrøder HD, Kassem M. Tumorigenic
589 heterogeneity in cancer stem cells evolved from long-term cultures of telomerase-immortalized
590 human mesenchymal stem cells. Cancer Res. 2005;65:3126–35.
591 34. van der Valk J, Brunner D, De Smet K, Fex Svenningsen A, Honegger P, Knudsen LE, Lindl T,
592 Noraberg J, Price A, Scarino ML, Gstraunthaler G. Optimization of chemically defined cell culture
593 media--replacing fetal bovine serum in mammalian in vitro methods. Toxicol In Vitro.
594 2010;24:1053–63.
595 35. Lukáš J, Richau K, Schwarz H-H, Paul D. Surface characterization of polyelectrolyte complex
596 membranes based on sodium cellulose sulfate and poly(dimethyldiallylammonium chloride). J Am
597 Coll Cardiol. 1995;106:281–8.
598 36. Lukáš J, Richau K, Schwarz H-H, Paul D. Surface characterization of polyelectrolyte complex
599 membranes based on sodium cellulose sulfate and various cationic components. Journal of
600 Membrane Science. 1997;131:39–47.
601 37. Zhang J, Yao S-J, Guan Y-X. Preparation of macroporous sodium cellulose
602 sulphate/poly(dimethyldiallylammonium chloride) capsules and their characteristics. Journal of
603 Membrane Science. 2005;255:89–98.
604 38. Dautzenberg H, Schuldt U, Lerche D, Woehlecke H, Ehwald R. Size exclusion properties of
605 polyelectrolyte complex microcapsules prepared from sodium cellulose sulphate and poly
606 [diallyldimethylammonium chloride]. Journal of Membrane Science. Elsevier; 1999;162:165–71.
607 39. Wu FT, Stefanini MO, Mac Gabhann F, Popel AS. A compartment model of VEGF distribution in
608 humans in the presence of soluble VEGF receptor-1 acting as a ligand trap. PLoS ONE. Public
609 Library of Science; 2009;4:e5108.
610 40. Brunner D, Frank J, Appl H, Schöffl H, Pfaller W, Gstraunthaler G. Serum-free cell culture: the

serum-free media interactive online database. ALTEX. 2010;27:53–62.
41. Liu S-Y, Chen C-L, Yang T-T, Huang W-C, Hsieh C-Y, Shen W-J, Tsai T-T, Shieh C-C, Lin C-F. Albumin prevents reactive oxygen species-induced mitochondrial damage, autophagy, and apoptosis during serum starvation. Apoptosis. Springer US; 2012;17:1156–69.
42. Bourdon E, Loreau N, BLACHE D. Glucose and free radicals impair the antioxidant properties of serum albumin. FASEB J. FASEB; 1999;13:233–44.

FIGURE LEGENDS

Figure 1. Chemical and morphological characterization of microcapsules. A) Schematic representation of microcapsule made of SCS and pDADMAC to encapsulate cells. B) Ultrastructure of microcapsules visualized using Back Scattered Electron Mode (BES) scanning electron microscopy (SEM). C) Microcapsule visualized using standard SEM protocol showing the loss of the liquid core after dehydration process. D) FTIR spectrum of naïve SCS and pDADMAC, and PEC formed after polymerization. E) Representative graph of microcapsule size distribution.

Figure 2. Behavior of primary hMSCs encapsulated in SCS-pDADMAC microcapsules. A) CLSM images showing viability of encapsulated cells stained with Calcein AM (green fluorescence indicates living cells) and Ethidium Homodimer-1 (EthD-1, red fluorescence indicates dead cells). Control dead cells were visualized using excitation and emission wavelengths of ~528nm/~617nm (dead cells) and ~495 nm/~515 nm (live cells). B) Metabolic activity using AlamarBlue® assay at days 0, 3, 7 and 14 post-encapsulation. Absorbance was measured at 550 and 595nm. Statistical analysis by one-way ANOVA with Tukey's multiple comparison test (*p<0.05 and **p<0.01 compared to day 0). C) Orthographic projection of microcapsules showing the localization of hMSCs inside of microcapsules. Cells were stained with Calcein AM and EthD-1. D) Cytoskeleton organization of encapsulated hMSCs stained with Phalloidin-FITC (green) for F-actin and propidium iodide (red) for nucleus.

Figure 3. **Biological response of primary hMSCs to microcapsule material measured by AlamarBlue® assay.** A) Cytotoxicity analysis of microcapsule components to hMSCs by direct contact with sterile empty microcapsules (direct contact), by contact with extracts of the device through diffusion (indirect contact) and by direct contact with 2% and 4% (w/v) SCS at 1:3 and 2:3 ratios (SCS:complete medium). Statistical analysis performed by unpaired Student's *t*-test (n.s.). B) CLSM images using transmitted laser light (TL) and LIVE/DEAD dyes (ZP: z projection and OP: orthographic projection) showing spreading of primary hMSC on the outer microcapsule membrane immediately and 24h after cell seeding. Statistical analysis performed by one-way ANOVA with Dunnett's multiple comparison test (n.s.).

Figure 4. Behavior of immortalized hMSC-TERT cells encapsulated in SCS-pDADMAC microcapsules. A) CLSM images showing viability of encapsulated cells stained with Calcein

AM (green fluorescence indicates live cells) and Ethidium Homodimer-1 (EthD-1, red fluorescence indicates dead cells). B) Metabolic activity using AlamarBlue® assay at days 0, 3, 7 and 14 post-encapsulation. Absorbance was measured at 550 and 595nm. Statistical analysis by one-way ANOVA with Tukey's multiple comparison test (n.s.). C) Orthographic projection of microcapsules showing the localization of hMSC-TERT cells inside of microcapsules. Cells were stained with Calcein AM and EthD-1. D) Cytoskeleton organization of encapsulated hMSC-TERT cells stained with Phalloidin-FITC (green) for F-actin and propidium iodide (red) for nuclei.

Figure 5. Diffusion properties of microcapsule membrane. A) SEM images of microcapsule membrane. Left image is the surface of microcapsule membrane; center image is a higher magnification of left image; right image shows a transverse section of a microcapsule membrane. B) CLSM images of microcapsules incubated with FITC- labeled dextrans of 10, 20 and 70kDa (with hydrodynamic radius R_h of 2.3 nm, 3,2 nm and 5.8 nm, respectively), FITC-coupled BSA (66.5 kDa, R_h 3.48 nm) and FITC-coupled chicken immunoglobulin IgY (180 kDa, R_h>5.5 nm).

Figure 6. Influence of macromolecular components from culture medium on primary hMSCs and hMSC-TERT growth. A) Protein composition of serum-free medium (lane 1), complete medium (lane 2), 50K-depleted medium (lane 3) and 50K-concentrated medium (lane 4) by SDS-PAGE and silver staining. B) Growth curve of primary hMSCs and hMSC-TERT cells cultured in complete medium —■—, serum-free medium --●--, 50K-depleted medium ⋯▲⋯ and 50K-concentrated medium ---·▼--·. C) Fold-change of primary hMSCs (**p<0.01 significance compared to complete medium) and hMSC-TERT growth (***p<0.001 compared to complete medium; +++ p<0.001 compared to serum-free medium and 50K-depleted medium) at day 9 compared to day 0. Dotted line at 1 represents baseline (day 0). Statistical significance by one-way ANOVA with Tukey's multiple comparison test.

Figure 7. *In vitro* angiogenic potential of encapsulated cells. A) Images of HUVECs tubule formation in matrigel after 14h incubation with EGM (positive control) EBM (negative control) and conditioned media from encapsulated hMSC-TERT cells and primary hMSCs 7 days post-encapsulation. B) Quantification of tubule-like structures 7 days post-encapsulation. Results are represented as fold-change compared to EGM. Statistical analysis by one-way ANOVA with Tukey's multiple comparison test (*p<0.05 and **p<0.01 significance compared to EBM,

678 +++p<0.001 significance compared to EGM). C) Quantification of VEGF levels released from
679 encapsulated cells 7 days post-encapsulation over a period of 24h, 48h and72 h by ELISA
680 (unpaired Student's *t*-test *p<0.05 and **p<0.01 significance of hMSC-TERT compared to
681 primary hMSC; two-way ANOVA with Tukey's test +p<0.05 significance of hMSC-TERT at 72
682 h compared to 24 h).

683 **Supporting information.** Three-dimensional simulation of microcapsule containing primary
684 hMSCs and hMSC-TERT cells (Video S1 and Video S2), characterization of primary hMSC by
685 flow cytometry and tri-lineage differentiation (Figure S1) morphology of primary hMSCs and
686 hMSC-TERT cells under CLSM (Figure S2), viability of other cell types (Figure S3),
687 fluorescence intensity spectrum (Figure S4) and quantification of VEGF levels from non-
688 encapsulated cells (Figure S5).

689

690 **List of Figures:**

691

692 **Figure 1**

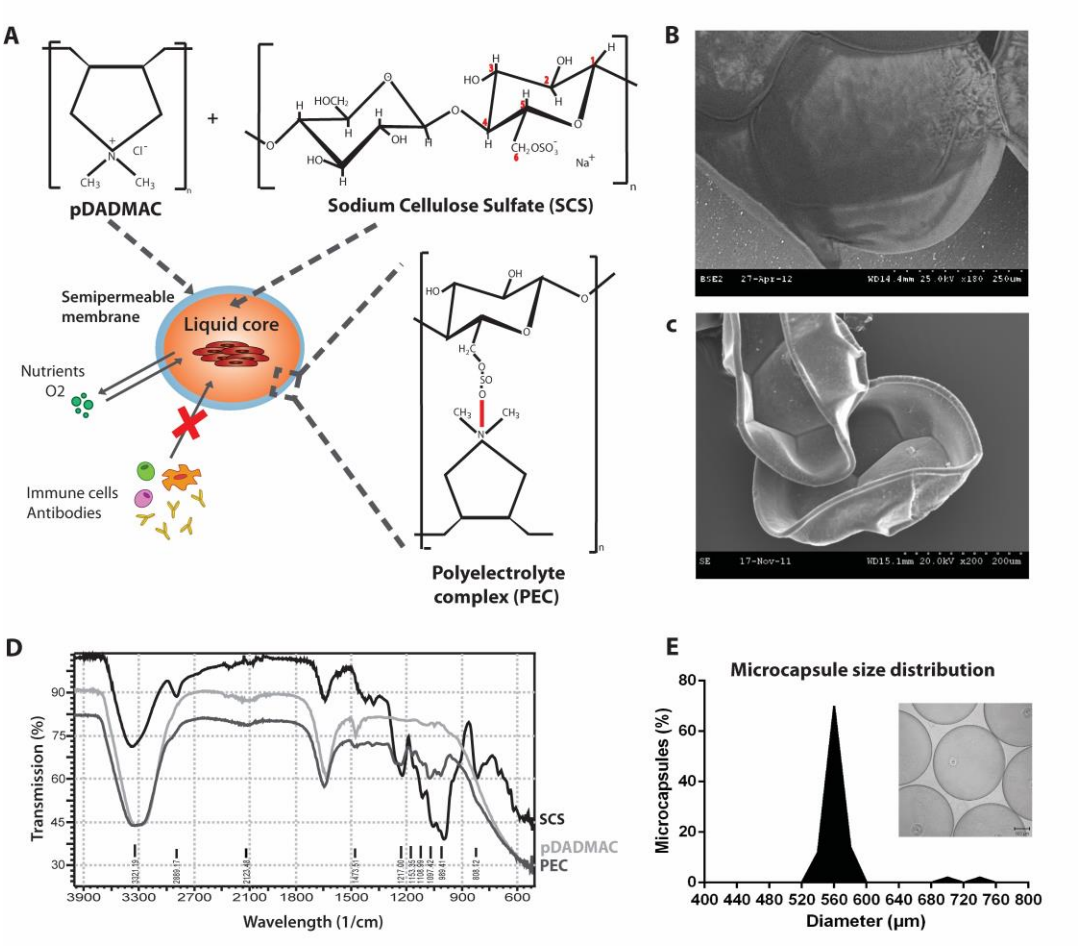

693

Figure 2

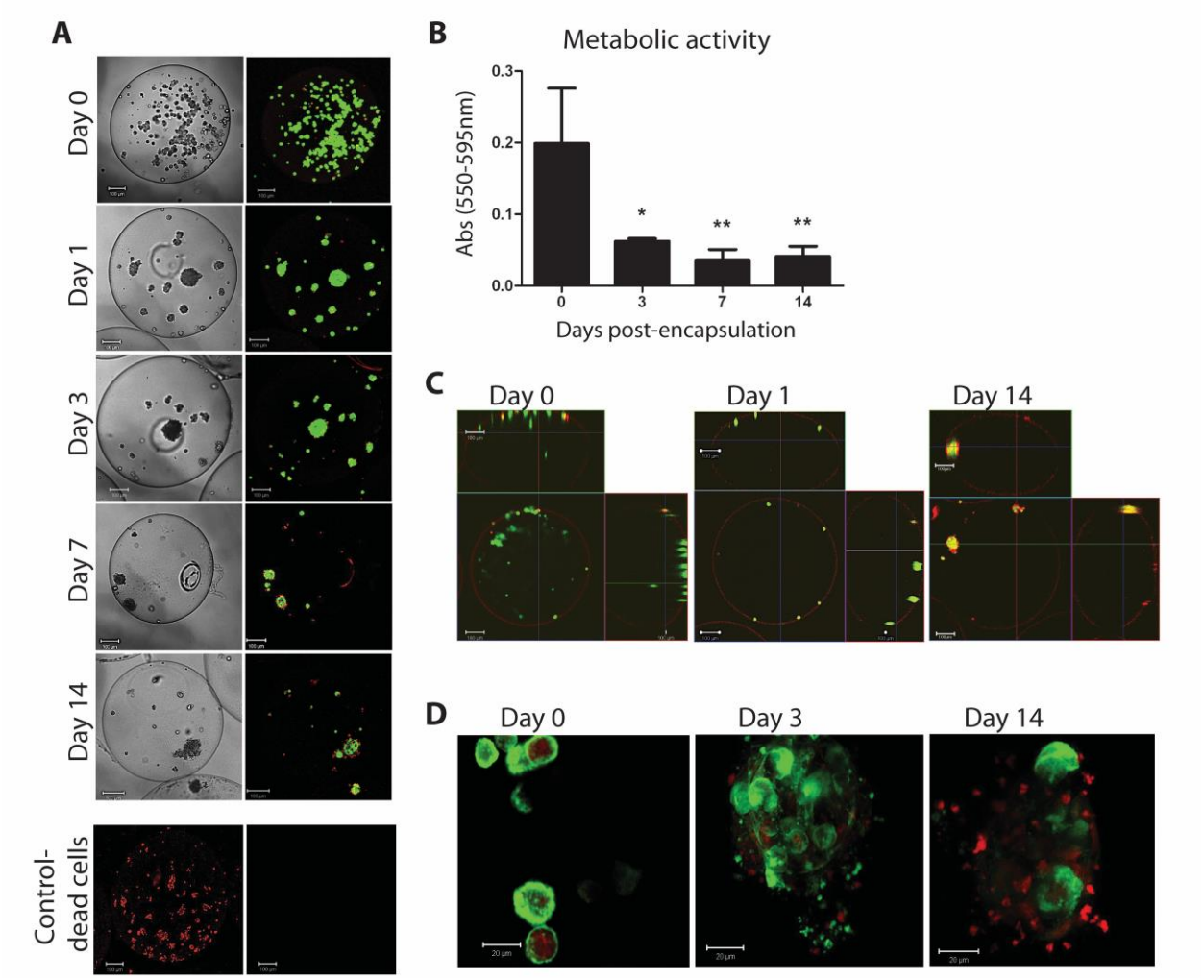
A
Day 0
Day 1
Day 3
Day 7
Day 14
Control-dead cells
B
Metabolic activity
Abs (550-595nm)
0.3
0.2
0.1
0.0
*
**
**
0
3
7
14
Days post-encapsulation
C
Day 0
Day 1
Day 14
D
Day 0
Day 3
Day 14

Figure 3

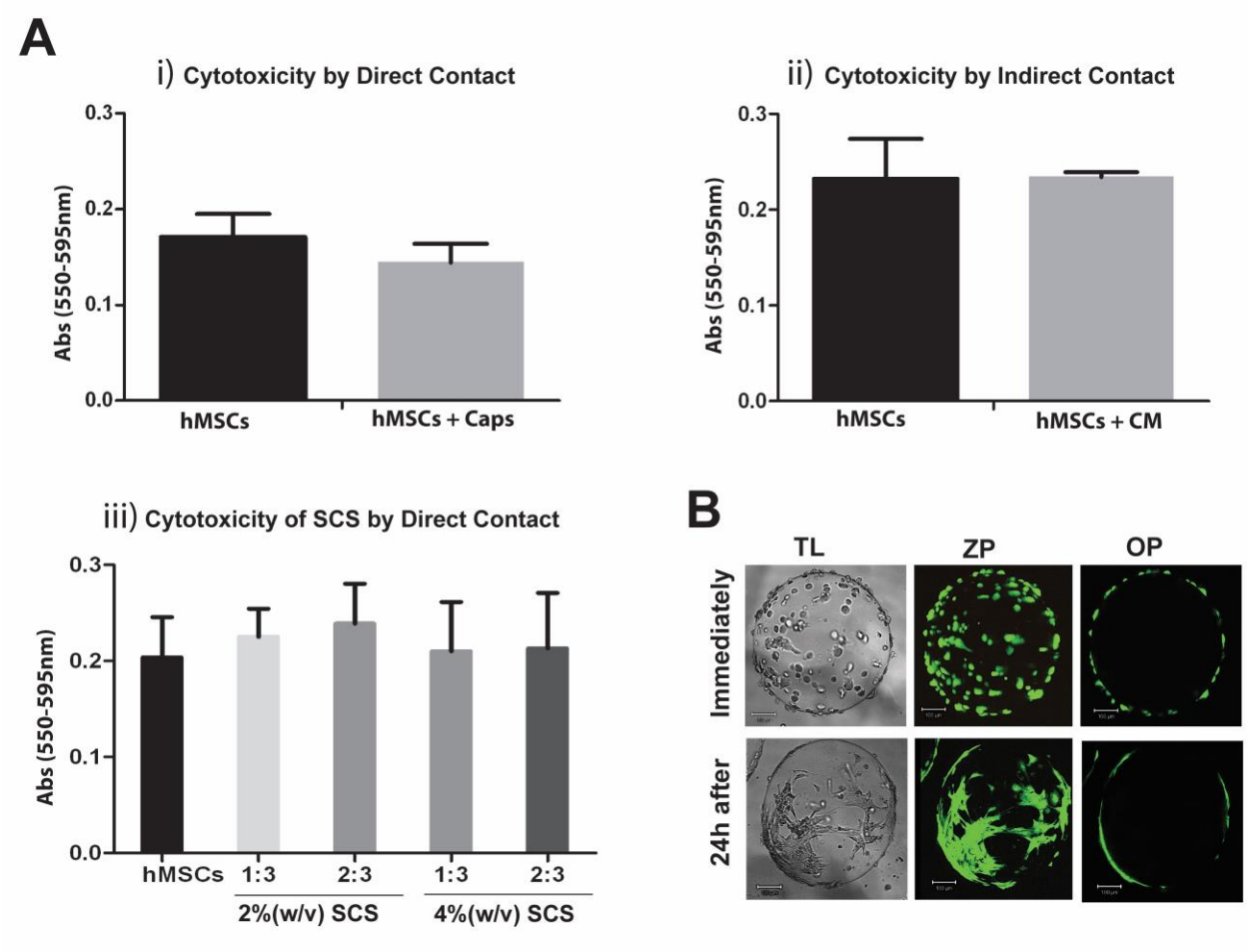
A
i) Cytotoxicity by Direct Contact
Abs (550-595nm)
0.3
0.2
0.1
0.0
hMSCs
hMSCs + Caps
ii) Cytotoxicity by Indirect Contact
Abs (550-595nm)
0.3
0.2
0.1
0.0
hMSCs
hMSCs + CM
iii) Cytotoxicity of SCS by Direct Contact
Abs (550-595nm)
0.3
0.2
0.1
0.0
hMSCs
1:3
2:3
1:3
2:3
2%(w/v) SCS
4%(w/v) SCS
B
TL
ZP
OP
Immediately
24h after

Figure 4

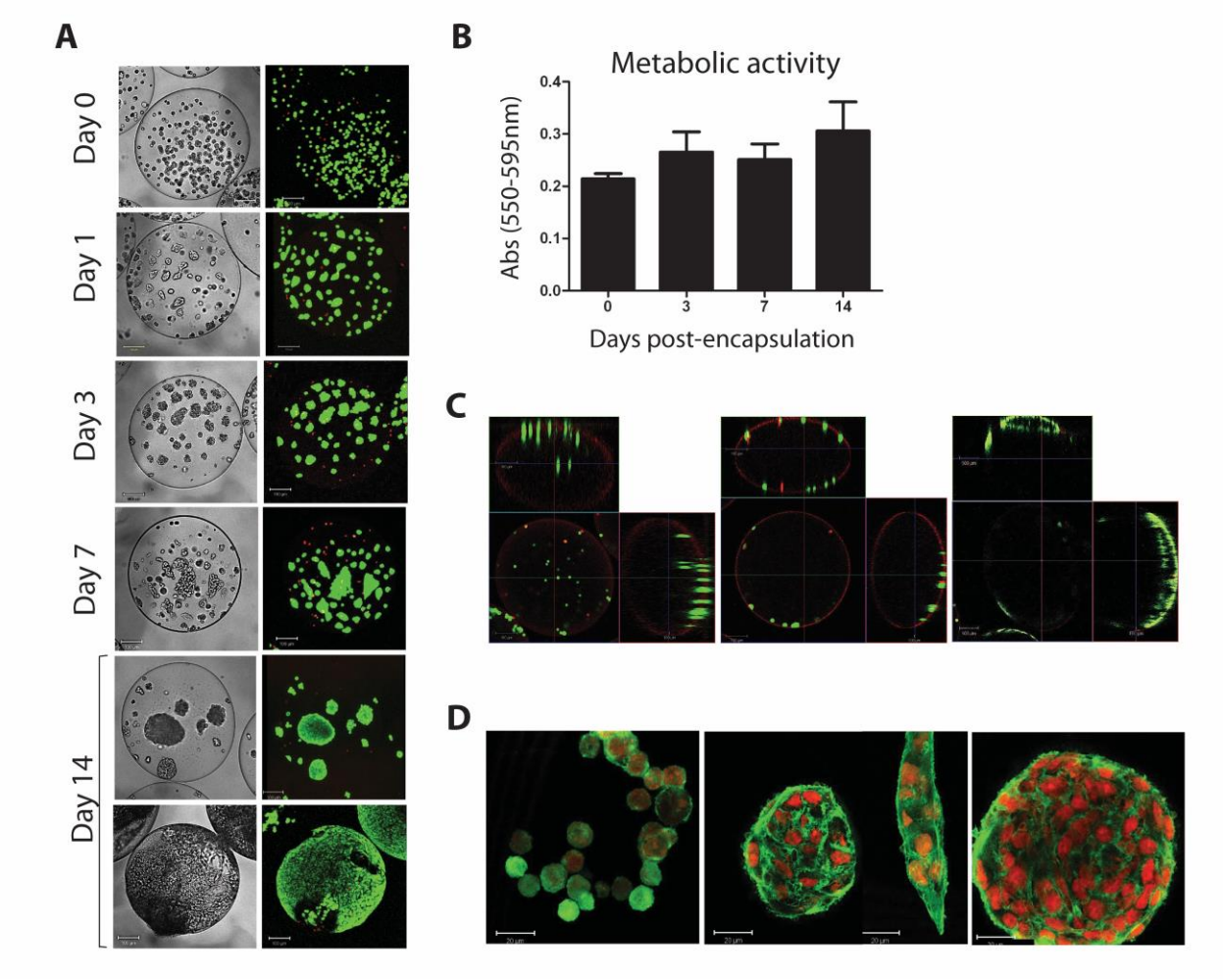
A
Day 0
Day 1
Day 3
Day 7
Day 14
B
Metabolic activity
Abs (550-595nm)
0.4
0.3
0.2
0.1
0.0
0
3
7
14
Days post-encapsulation
C
D

Figure 5

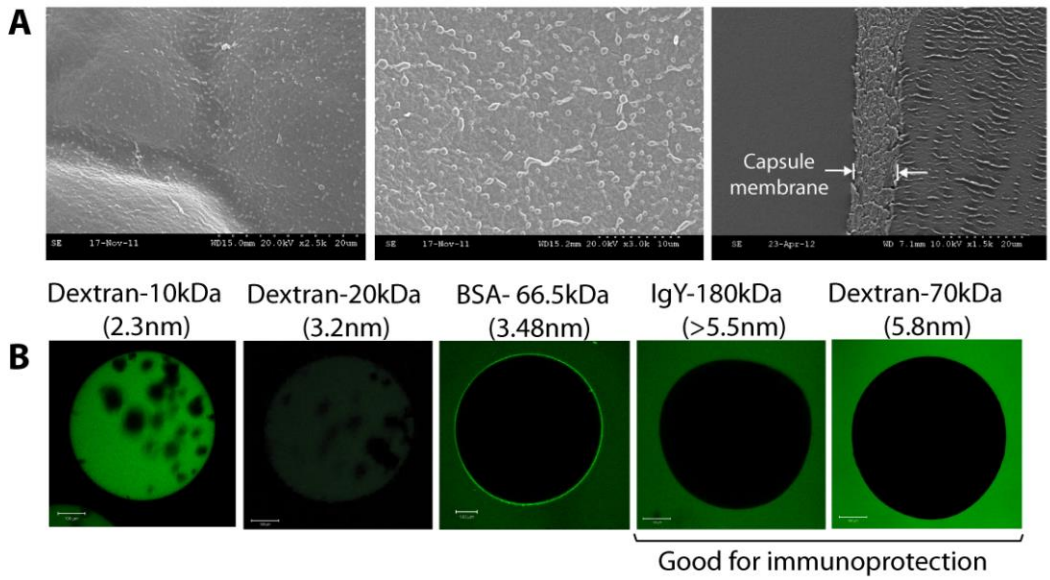
A
Capsule membrane
Dextran-10kDa (2.3nm)
Dextran-20kDa (3.2nm)
BSA- 66.5kDa (3.48nm)
IgY-180kDa (>5.5nm)
Dextran-70kDa (5.8nm)
B
Good for immunoprotection

Figure 6

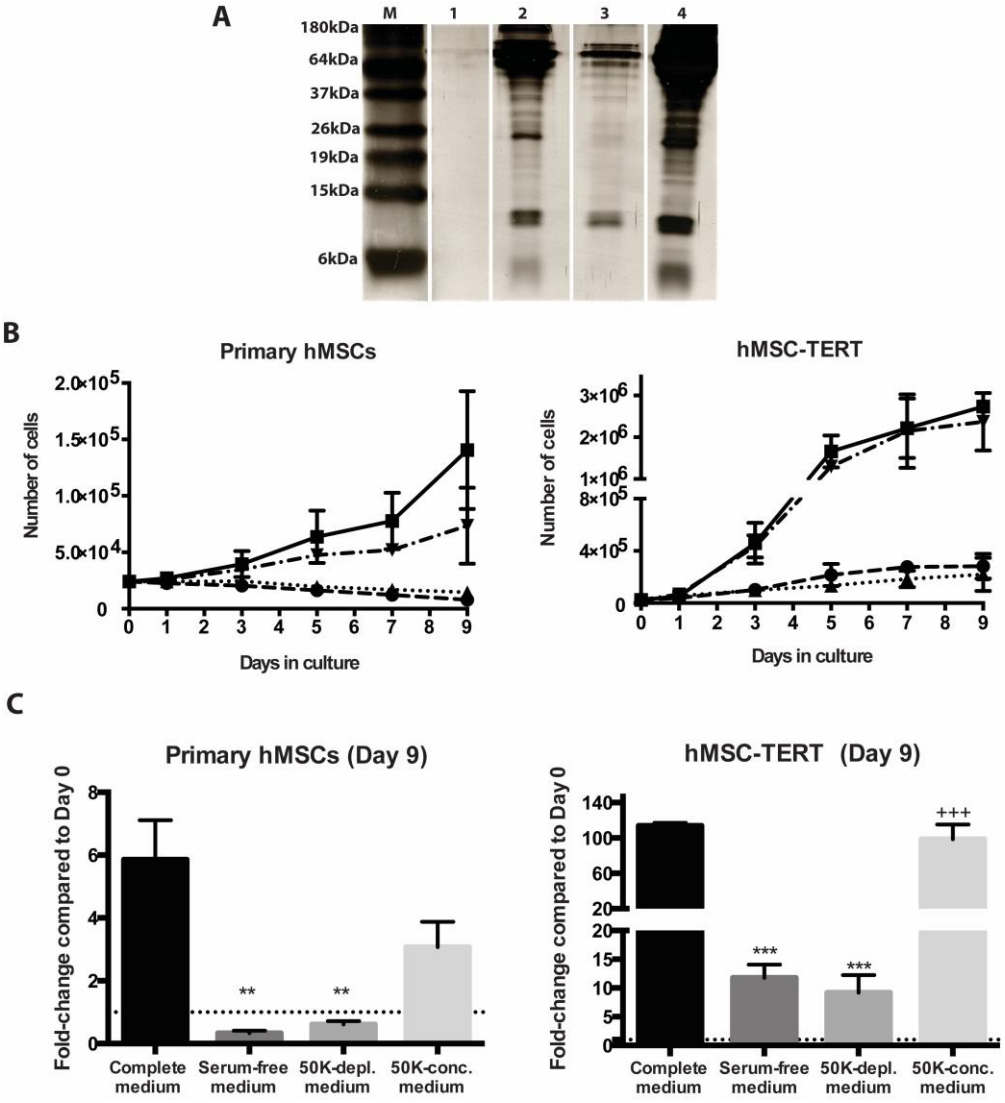
A
M
1
2
3
4
180kDa
64kDa
37kDa
26kDa
19kDa
15kDa
6kDa
B
Primary hMSCs
hMSC-TERT
Number of cells
Days in culture
C
Primary hMSCs (Day 9)
hMSC-TERT (Day 9)
Fold-change compared to Day 0
Complete medium
Serum-free medium
50K-depl. medium
50K-conc. medium

715 **Figure 7**

716

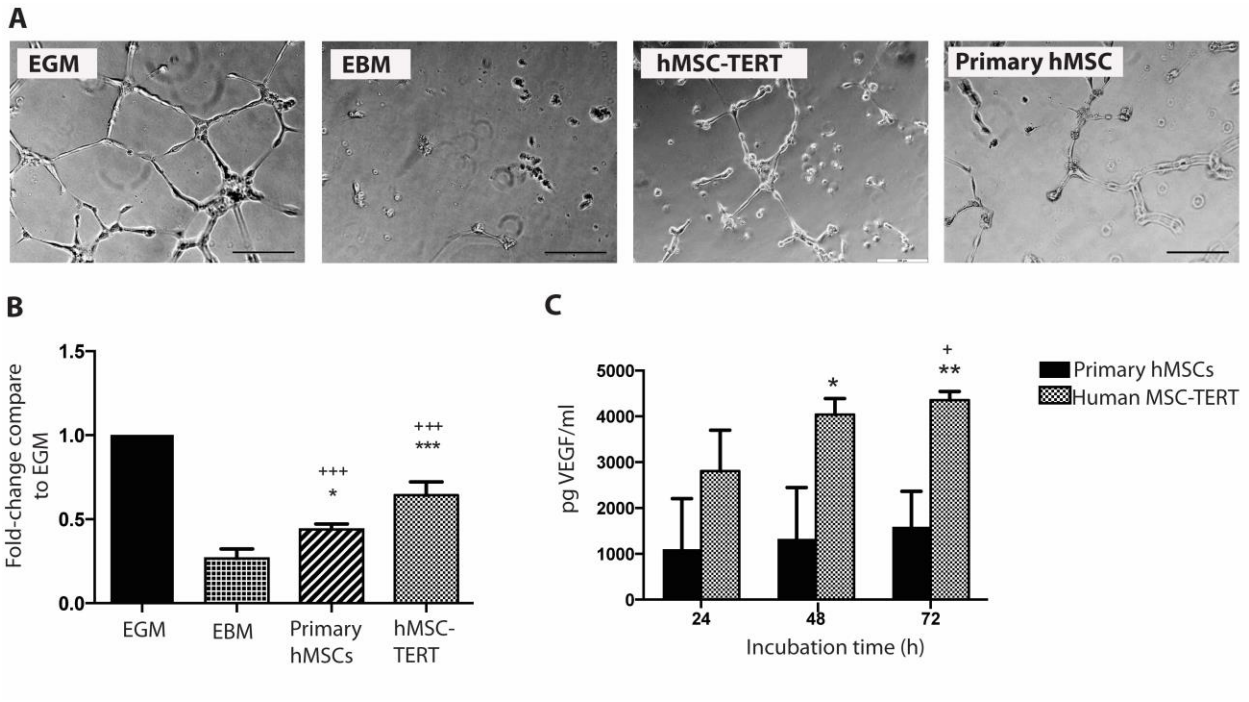

717